AAEC/E379

AAEC/E379

AUSTRALIAN ATOMIC ENERGY COMMISSION

RESEARCH ESTABLISHMENT

LUCAS HEIGHTS

THE ACCURACY OF THE DIFFUSION THEORY COMPONENT OF REMOVAL-DIFFUSION THEORY

by

I.J. DONNELLY

March 1976
ISBN O 642 99730 6

AUSTRALIAN ATOMIC ENERGY COMMISSION
RESEARCH ESTABLISHMENT
LUCAS HEIGHTS

THE ACCURACY OF THE DIFFUSION THEORY COMPONENT OF REMOVAL-DIFFUSION THEORY

by

I.J. DONNELLY

ABSTRACT

The neutron fluxes in five neutron shields consisting of water, concrete, graphite, iron and an iron-water lattice respectively, have been calculated using P_1 theory, diffusion theory with the usual transport correction for anisotropic scattering (DT), and diffusion theory with a diagonal transport correction (DDT). The calculations have been repeated using transport theory for the flux above 0.5 MeV and the diffusion theories for lower energies. Comparisons with transport theory calculations reveal the accuracy of each diffusion theory when it is used for flux evaluation at all energies, and also its accuracy when used for flux evaluation below 0.5 MeV given the correct flux above 0.5 MeV. It is concluded that the diffusion component of removal-diffusion theory has adequate accuracy unless the high energy diffusion flux entering the shield is significantly larger than the removal flux. In general, P_1 and DT are more accurate than DDT and give similar fluxes except for shields having a large hydrogen content, in which case DT is better. Therefore it is recommended that DT be used in preference to P_1 theory or DDT.

National Library of Australia card number and ISBN 0 642 99730 6

The following descriptors have been selected from the INIS Thesaurus to describe the subject content of this report for information retrieval purposes. For further details please refer to IAEA-INIS-12(INIS: Manual for Indexing) and IAEA-INIS-13 (INIS: Thesaurus) published in Vienna by the International Atomic Energy Agency.

CONCRETES; GRAPHITE; IRON; MATHEMATICAL MODELS; MULTIGROUP THEORY; NEUTRON DIFFUSION EQUATION; NEUTRON DOSIMETRY; NEUTRON FLUX; NEUTRONS; SHIELDING MATERIALS; SHIELDS; SIMULATION; WATER

CONTENTS

CONTENTS (Continued)

1. INTRODUCTION

The removal-diffusion method is commonly used to perform calculations of the neutron flux in one- and two-dimensional neutron shields. It has the advantage of being cheaper to use than transport theory methods and experience has shown that it has adequate accuracy for the calculation of many shield configurations, especially when the shield materials contain hydrogen. In this report the diffusion part of removal-diffusion theory has been tested to see if more accurate results can be obtained when it is replaced either by P_1 theory or by diagonal diffusion theory.

No general statement which will apply to all shielding configurations can be made about the accuracy of the various methods examined. The best approach is either to investigate in detail a specific shield of interest, or to select a range of the most common shielding materials in some standard shield configuration and find the accuracy of each method for these general cases. Several authors have used one or the other of these procedures, usually to obtain a comparison between transport and diffusion theories; Sahin [1973] lists several of these investigations. The second approach has been taken for this work.

A one-dimensional plane geometry has been used to specify the shields, which are composed of either water, concrete, graphite, iron or an iron-water lattice. A neutron source was imposed on the left hand side of each shield, and the neutron flux through the shield was calculated using each of the diffusion theory approximations examined. A transport theory calculation was also performed to allow an assessment of the accuracy of the approximate methods. All calculations were made using the code ANISN [Engle 1967] with cross sections taken from the FARS [RSIC Computer Code Collection 1969] library. To simplify the analysis of results, several integral quantities of interest, such as biological dose, have been computed from the diffusion theory fluxes, and their values compared with those given by transport theory.

A brief description of removal-diffusion theory is given in Sections 2 and 3, along with a description of the approach used in this study to separate the 'removal' and 'diffusion' neutrons so that an evaluation of the various approximate treatments of the latter can be made. In Section 4, the three diffusion theories are compared analytically to aid in the interpretation of the numerical results. For the same reason, a one-group comparison of transport and diffusion theory is made in Section 5. The results of the numerical calculations and comparisons of the diffusion

theories are discussed in Section 7, followed by a summary of the major conclusions.

2. REMOVAL - DIFFUSION THEORY

Removal-diffusion theory [Price *et al.* 1957] is based upon the observation that in many shields, particularly those containing hydrogen, the neutron flux is determined by the high energy (E > 0.5 MeV) component of the flux. Therefore, an accurate calculation of the high energy flux (which can be performed in many cases using a combination of removal and diffusion theories), plus a diffusion theory evaluation of the flux at lower energies, leads to reasonably accurate flux values.

A brief outline of a removal-diffusion theory calculation is now given, with emphasis upon the role played by diffusion theory. For further details see, for example, the description of the SABINE code by Ponti & Van Heusden [1974].

(i) Most removal-diffusion codes need, as input data, the spatial distribution of the fission rate throughout the reactor core and the energy-dependent neutron flux at the inner boundary of the shield, so these quantities are determined before the removal-diffusion calculation.

(ii) The removal flux is calculated throughout the shield. The removal flux at a given point is composed of the neutrons which are produced in fissions throughout the reactor and reach the point without having suffered a collision. The collision cross section for these neutrons is called the removal cross section. It is approximately equal to the transport cross section. Several methods have been developed for the evaluation of removal cross sections (see, for example, Ponti & Van Heusden [1974] and Tanaka *et al.* [1972]).

(iii) As the removal neutrons move through the shield, they are scattered out of the removal flux. The scattering rate of the removal neutrons is calculated, and used as a source of diffusion neutrons in the diffusion theory calculation in step (v).

(iv) The neutron flux at the inner boundary of the shield is composed of both removal and non-removal neutrons and, as the removal component has been calculated in step (ii), the non-removal component can be obtained from the flux values specified at the inner boundary of the shield. This non-removal flux at the inner boundary of the shield gives one boundary condition for the

diffusion theory calculation. The other boundary condition generally takes the form of a vacuum or albedo condition at the outer boundary of the shield.

(v) The non-removal flux in the shield is calculated using diffusion theory, with the source described in (iii) and the boundary conditions described in (iv).

(vi) The neutron flux in the shield is the sum of the removal flux and the diffusion theory flux.

3. THE SIMULATION OF A REMOVAL-DIFFUSION CALCULATION

The following procedure has been used to assess the accuracy of the diffusion, P_1, and diagonal diffusion theories when they are used to evaluate the non-removal flux.

(i) A transport theory calculation of the neutron flux in each shield is performed.

(ii) The neutron flux is calculated using transport theory for energies greater than 0.5 MeV, and using each of the diffusion theories for energies below 0.5 MeV. The accuracy of the diffusion theories for the evaluation of the flux below 0.5 MeV, given accurate flux values above 0.5 MeV, is then found by comparison with step (i) flux values.

(iii) The flux is calculated using each of the diffusion theories, and their accuracy is found by comparison with step (i) flux values.

Step (ii) allows an assessment of the accuracy of each diffusion theory for the evaluation of the non-removal flux component (below 0.5 MeV) coming from neutrons scattered out of the removal flux in the shield. Step (iii) allows an assessment of each diffusion theory for the evaluation of the non-removal flux component which enters the shield through its boundaries.

A few of the neutrons that are scattered out of the removal flux have an energy above 0.5 MeV and they undergo several more collisions before their energy is reduced below this value. The accuracy of diffusion theory for the calculation of these neutrons has not been explicitly evaluated in this study. However, it can be inferred from the results obtained in steps (ii) and (iii) that the inclusion of these neutrons in the diffusion theory calculation in step (ii) would not alter the conclusions reached regarding the accuracy of each diffusion theory.

This procedure, while only an approximation to a removal-diffusion calculation, allows an assessment of the accuracy of each of the diffusion

theories in the roles which they would have to play in a removal-diffusion calculation.

4. A COMPARISON OF THE P_1 AND DIFFUSION THEORY EQUATIONS

The multigroup P_1 and the two multigroup diffusion theory equations are now compared assuming plane geometry. This analysis of the relationship between the three methods helps in the interpretation of the numerical experiments discussed later.

In plane geometry, the G-group transport equation for group g is

$$\mu \frac{\partial \psi_g(x,\mu)}{\partial x} + \sigma_g \psi_g(x,\mu) = \tfrac{1}{2} \sum_{\ell=0}^{L} \sum_{g'=1}^{G} (2\ell+1) \left[\sigma_{\ell,g' \to g} \phi_{\ell,g'}(x) + Q_\ell(x) \delta_{gg'} \right] P_\ell(\mu) \quad . \qquad \ldots(1)$$

The notation and following analysis is similar to that of Bell & Glasstone [1970]. The P_1 multigroup approximation to Equation (1) is attained by multiplying the equation by $P_n(\mu)$, integrating over μ for n = 0 and n = 1, and putting $\phi_{\ell,g'}(x) \equiv 0$ for $\ell > 1$. This results in the equations

$$\frac{dj_g(x)}{dx} + \sigma_g \phi_g(x) = \sum_{g'=1}^{G} \sigma_{o,g' \to g} \phi_{g'}(x) + Q_{o,g}(x) \qquad \ldots(2a)$$

and

$$\frac{1}{3} \frac{d\phi_g(x)}{dx} + \sigma_g j_g(x) = \sum_{g'=1}^{G} \sigma_{1,g' \to g} j_{g'}(x) + Q_{1,g}(x) \quad , \qquad \ldots(2b)$$

where $\phi_g \equiv \phi_{o,g}$ and $j_g \equiv \phi_{1,g}$. In the later numerical work $Q_{1,g}(x) = 0$, so this is assumed henceforth. Equation (2a) may be expressed in the usual diffusion theory form

$$-\frac{d}{dx} \left[D_g(x) \frac{d\phi_g(x)}{dx} \right] + \sigma_g \phi_g(x) = \sum_{g'=1}^{G} \sigma_{o,g \to g} \phi_{g'}(x) + Q_g(x) \quad , \ldots(3)$$

where the P_1 form of the diffusion coefficient, as obtained from Equation (2b), is

$$P_1: \quad D_g(x) = \frac{1}{3}\left[\sigma_g - \sum_{g'=1}^{G} \sigma_{1,g'\to g} j_{g'}(x)/j_g(x)\right]^{-1} . \qquad \ldots(4)$$

The other two diffusion theories also obey Equation (3), but have different definitions of the diffusion coefficient. The most common version of diffusion theory (DT) incorporates a correction for anisotropic scattering which can be derived from the first order form of the extended transport approximation to the scattering function, as defined by Bell *et al.* [1967]. This leads to the following diffusion coefficient,

$$DT: \quad D_g(x) = \frac{1}{3}\left[\sigma_g - \sigma_{1,g}\right]^{-1} , \qquad \ldots(5)$$

where

$$\sigma_{1,g} = \sum_{g'=1}^{G} \sigma_{1,g\to g'} . \qquad \ldots(6)$$

Pendlebury & Underhill [1962] have considered a within group approximation to the scattering function. The version of diffusion theory associated with this approximation is called diagonal diffusion theory (DDT), and it has the following diffusion coefficient,

$$DDT: \quad D_g(x) = \frac{1}{3}\left[\sigma_g - \sigma_{1,g\to g}\right]^{-1} . \qquad \ldots(7)$$

A few brief comments are now made on the relationships between the three theories:

(i) All theories are the same when the anisotropic scattering is small.

(ii) For a coarse energy group structure, $\sigma_{1,g} \triangleq \sigma_{1,g\to g}$ and the three theories are the same.

(iii) For a fine energy group structure, $\sigma_{1,g\to g} \triangleq 0$, so DDT has little correction for anisotropic scattering.

(iv) Bell & Glasstone [1970] have pointed out that

$$\sum_{g'=1}^{G} \sigma_{1,g'\to g} j_{g'} \triangleq \sigma_{1,g} j_g \qquad \ldots(8)$$

as long as $\xi_1(u)\sigma_1(u)j(u)$ has little variation over group g;

the term $\sigma_1(u) = \int_u^\infty \sigma_1(u \to u')du'$ and $\xi_1(u)$ is the P_1 component of the average lethargy loss per collision at lethargy u; that is

$$\xi_1(u) = \int_u^\infty (u'-u)\sigma_1(u \to u')du'/\sigma_1(u) \quad .$$

Equation (8) is generally a reasonable approximation, except perhaps for light nuclei which have a large value of ξ_1. Substitution of Equation (8) into Equation (4) reduces the P_1 diffusion coefficient to that for DT, so the P_1 and DT theories will give similar results in shielding materials for which Equation (8) is valid.

5. A ONE-GROUP COMPARISON OF TRANSPORT AND DIFFUSION THEORY

The interpretation of the numerical results is aided by the following one-group comparison of transport and diffusion theory for a homogeneous, plane geometry shield.

In typical shielding problems with only one thermal group, there is no neutron upscatter and no fission sources in the shield; the G-group transport equations, given in Equation (1), can be written therefore as G one-group equations, each one of the form

$$\mu \frac{\partial\psi(x,\mu)}{\partial x} + \sigma\psi(x,\mu) = \frac{1}{2}\sum_{\ell=0}^{L}(2\ell+1)\left[\sigma_\ell\phi_\ell(x) + Q_\ell(x)\right]P_\ell(\mu), \quad \ldots(10)$$

where the source $Q_\ell(x)$ consists of both an external source and a downscatter source from higher energy groups. The following analysis of the one-group flux is made assuming isotropic scattering. Anisotropic scattering may be approximately included by use of the transport approximation in which σ is replaced by $\sigma-\sigma_1$ and σ_o by $\sigma_o-\sigma_1$. Replacing σ_o by $c\sigma$, Equation (10) becomes

$$\mu \frac{\partial\psi(x,\mu)}{\partial x} + \sigma\psi(x,\mu) = \frac{1}{2}c\sigma\phi(x) + \frac{1}{2}Q(x) \quad . \qquad \ldots(11)$$

The diffusion theory approximation to this equation is

$$-D\frac{d^2\phi_d(x)}{dx^2} + (1-c)\sigma\phi_d(x) = Q(x) \quad . \qquad \ldots(12)$$

In the following analysis it is assumed that the flux $\psi(x,\mu)$ represents the flux below 0.5 MeV, and $Q(x)$ is the downscatter source coming from the flux above 0.5 MeV. In many shields it is found that the exponential function

$$Q(x) = Q\exp(-\kappa_s x) \qquad \ldots(13)$$

describes this source well. A source of this form suffices for this analysis.

Two situations of interest arise, depending on whether the eigenvalue κ derived from the homogeneous part of Equation (11) is less or greater than κ_s.

5.1 The Eigenvalue $\kappa < \kappa_s$

In this case, the flux $\phi(x)$ decreases less quickly with x than the source does, and it has the functional form

$$\phi(x) = \phi \exp(-\kappa x) \qquad \ldots(14)$$

for large x. Transport theory requires that κ satisfies the equation [Tait 1964a]

$$\frac{c\sigma}{\kappa} \tanh^{-1}\left[\frac{\kappa}{\sigma}\right] = 1 \quad , \qquad \ldots(15)$$

whereas the diffusion theory approximation results in an eigenvalue

$$\kappa_d = \left[(1-c)\sigma/D\right]^{\frac{1}{2}}$$

$$= \left[3(1-c)\right]^{\frac{1}{2}}\sigma \quad . \qquad \ldots(16)$$

It is well known that $\kappa_d > \kappa$, although they are similar for values of c near 1, (see Tait [1964b] for a comparison of κ_d with κ for varying c). It is therefore apparent that for $\kappa < \kappa_s$, diffusion theory will underestimate the neutron flux for large x. It is possible that $\kappa < \kappa_s < \kappa_d$; in this case $\phi_d(x) = \phi_d\exp(-\kappa_s x)$ and, once again, $\phi_d(x) < \phi(x)$ for large x.

5.2 The Eigenvalue $\kappa > \kappa_s$

In this case the flux is dominated by the source distribution and has the functional form

$$\phi(x) = \phi\exp(-\kappa_s x) \qquad \ldots(17)$$

for large x. An expression for ϕ can be obtained by substituting

$\psi(x,\mu) = \psi(\mu)\exp(-\kappa_s x)$ into Equation (11), dividing by $(\sigma-\mu\kappa_s)\exp(-\kappa_s x)$ and integrating over μ. Remembering that $\phi = \int_{-1}^{1} \psi(\mu)d\mu$, rearrangement of terms gives

$$\phi = \frac{Q \tanh^{-1}\left[\frac{\kappa_s}{\sigma}\right]}{\kappa_s - c\sigma\tanh^{-1}\left[\frac{\kappa_s}{\sigma}\right]} \quad . \qquad \ldots(18)$$

The diffusion theory flux has the functional form

$$\phi_d(x) = \phi_d \exp(-\kappa_s x) \qquad \ldots(19)$$

with

$$\phi_d = \frac{Q}{D(\kappa_d^2-\kappa_s^2)} \quad . \qquad \ldots(20)$$

The ratio of the amplitude of the diffusion theory flux to that of the transport theory flux is

$$R = \phi_d/\phi$$

$$= \frac{\kappa_s - c\sigma\tanh^{-1}\left[\frac{\kappa_s}{\sigma}\right]}{D(\kappa_d^2-\kappa_s^2)\tanh^{-1}\left[\frac{\kappa_s}{\sigma}\right]} \quad . \qquad \ldots(21)$$

The following analysis shows that $R < 1$. As $\kappa_s < \kappa$, there is a $c' > c$ such that

$$\frac{c'\sigma}{\kappa_s}\tanh^{-1}\left[\frac{\kappa_s}{\sigma}\right] = 1 \quad .$$

Substituting this into Equation (21), it follows, after some rearrangement of terms, that

$$R = \frac{3(c'-c)\sigma^2}{\kappa_d^2-\kappa_s^2} \quad .$$

Now $\kappa_d^2 = 3(1-c)\sigma^2$ and $\kappa_s^2 < 3(1-c')\sigma^2$, so

$$R = \frac{(1-c)-(1-c')}{(1-c)-\kappa_s^2/3\sigma^2}$$

$$< 1 \quad .$$

An expansion of Equation (21) in powers of κ_s/σ results in the expression

$$R = 1 - \frac{4\kappa_s^2}{15(\kappa_d^2-\kappa_s^2)} \cdot \left(\frac{\kappa_s}{\sigma}\right)^2 + 0\left(\left(\frac{\kappa_s}{\sigma}\right)^4\right). \qquad \ldots(22)$$

Thus, when the neutron flux is dominated by an exponentially decreasing source term, diffusion theory gives a smaller value for the flux than does transport theory. It can be deduced from the expressions obtained for R that, unless $\kappa \doteq \kappa_s$, the ratio of the diffusion to the transport theory flux is near unity.

6. DETAILS OF THE CALCULATIONAL METHODS

The shielding materials investigated are water, concrete, graphite, iron and an iron-water lattice. The shields calculated are one-dimensional plane geometry slabs, all of thickness 120 cm except for the graphite which has a thickness of 240 cm. Material compositions are listed in Table 1 and the dimensions of the iron-water lattice are given in Figure 1. The source used was spatially flat with a neutron fission spectrum; it occupied the first two centimetres on the left hand side of the shield. A reflecting boundary condition was applied to the left hand boundary of the shield and a vacuum boundary condition to the right hand boundary. All calculations were carried out using the transport theory code ANISN [Engle 1967] with a condensed version of the FARS neutron and gamma-ray cross section library [RSIC Computer Code Collection 1969]. The FARS cross sections for each material have been condensed using the ANISN generated flux spectrum resulting from a spatially constant, fission spectrum, neutron source in an infinite slab of the material. The condensed group structure contains 29 neutron groups and 11 gamma-ray groups (Table 2). The gamma-rays have been included in the calculations to allow an assessment of the effects of different methods of calculating the neutron flux (and hence the gamma-ray source distribution) on the gamma-ray flux levels in each shield. The gamma-ray fluxes were always calculated using transport theory.

The P_1 theory option in ANISN allowed the P_1, DT and DDT calculations to be carried out. The DT and DDT calculations required that the P_1 anisotropic downscatter cross sections be set equal to zero in the cross section library, and that the P_1 self-scatter term be set equal to $\sigma_{1,g}$ for DT calculations and left unaltered for the DDT calculations.

An S_8 version of transport theory with P_3 anisotropic scattering was used. The spatial mesh size was 2 cm except for the iron-water lattice, in which case a 1 cm mesh was taken. These quadrature and mesh sizes give fluxes which are accurate to within a few per cent for the problems analysed here.

The effect of geometry curvature has been evaluated by calculating the flux in a water sphere of radius 120 cm. The source was positioned at the centre with radius 2 cm; $S_{16}(P_3)$ transport theory and a 1 cm mesh were used.

7. RESULTS AND ANALYSIS OF THE NUMERICAL CALCULATIONS

The results obtained using the various calculational methods are now compared and analysed. The calculational methods are labelled transport, for a transport calculation in neutron groups 1 to 29; partial P_1, for a transport calculation in groups 1 to 12 and a P_1 calculation in groups 13 to 29; and total P_1, for a P_1 calculation in groups 1 to 29.

The comparisons made are of various integral quantities of the neutron or gamma-ray flux, namely, the neutron biological dose rate, the fast neutron flux $\phi_f(E > 1\ \text{MeV})$, the neutron flux just above thermal energies $\phi_{28}(0.414\ \text{eV} < E < 1.13\ \text{eV})$, the thermal neutron flux ϕ_{th} and the gamma-ray biological dose rate. For a given shield, only the more informative of these comparisons are discussed here. In assessing the partial diffusion theory calculations of the neutron dose, it should be borne in mind that the differences in predicted doses are solely due to differences in the neutron flux below 0.5 MeV.

In Figures 2 to 13, the results have been plotted in one of two ways, depending on the size of the errors in the diffusion theories. If the errors are small, then the percentage difference in each of the diffusion theories, relative to the transport theory, is plotted against x, the distance into the shield. The percentage difference is defined as

$$PD = (\text{Diffusion theory value}/\text{Transport theory value} - 1) \times 100\ \% \quad . \qquad \ldots(23)$$

If the errors are large, then the

$$\text{RATIO} = \text{Diffusion theory value/Transport theory value} \qquad \ldots(24)$$

is plotted on a logarithmic scale.

As an aid in the assessment of the importance of the differences in the fluxes, the transport theory flux and dose values have been normalised to unity at $x = 0$, and their values are given in Table 3 for each shield.

One consistent trend in the results (see Figures 3, 5, 7, 9, 10 and 12) is that the neutron fluxes predicted by the total diffusion theories tend to be too low for $x \triangleq 0$ cm, too large for $x \triangleq 10$ cm, and they become too small for large x. This is the type of behaviour that is predicted by a one-group comparison of transport and diffusion theory fluxes coming from an isotropic plane source (which is a reasonable approximation to the 2 cm source used here). The results that would be obtained with a wider source can be estimated, for the homogeneous shields, using the flux from the 2 cm source as a Green's function and integrating it over the desired source distribution. These considerations, plus a calculation of the water shield using a 10 cm wide source, show that with the wider source the oscillation in the diffusion theory fluxes near $x = 0$ cm are damped and better accuracy is obtained, but the trends in the flux behaviour for $x > 20$ cm remain much the same.

The results of the calculations are now discussed for each shield in turn.

7.1 The Water Shield

Figure 2 shows a plot of PD for the partial diffusion theory neutron doses. Note that the partial DDT values are ten times as large as shown. It is apparent that the partial P_1 and DT theories are quite accurate. The PD values for the thermal neutron fluxes show a spatial variation similar to that of the neutron dose PD values, except that the former are about five times larger; for example, at $x = 50$ cm, PD (partial P_1) = -0.28%, PD (Partial DT) = -4.63% and PD (Partial DDT) = -12.01%. Neutron doses evaluated for the spherical shield, using the partial diffusion methods, show PD values very similar to those obtained for the plane shield (with the radius coordinate r replacing x), except for $r < 20$ cm when the errors are up to four times as large.

Figure 3 shows the RATIO values of the neutron doses obtained using the total diffusion theories. It is apparent that both total P_1 and total

DDT doses become much too small with increasing x, while the total DT doses are 50 per cent too large for $x \triangleq 50$ cm, nearly correct for $x \triangleq 90$ cm and too small for large x. The thermal neutron fluxes exhibit a similar behaviour. Neutron doses evaluated for the spherical shield using the total diffusion methods give RATIO values similar to those obtained for the plane shield, and for $r > 20$ cm the RATIO graph for the spherical water shield appears similar to that for the plane water shield (Figure 3). This is to be expected, since the plane shield fluxes can be derived to a good approximation from the spherical shield fluxes using the Green's function method.

The gamma-ray doses are predicted to within a few per cent by each theory. This is due to the long mean free path of gamma-rays in water, which means that the gamma-ray dose depends predominantly on the neutron flux near $x = 0$ cm and is, therefore, insensitive to the neutron flux in other parts of the shield.

The excessively fast attenuation of the neutron flux predicted by the total diffusion theories, coupled with the accuracy of the partial diffusion theories, indicates that the neutron attenuation in water is governed by the behaviour of the fast neutrons ($E > 0.5$ MeV). The partial diffusion theory calculations therefore correspond to the one-group analysis with $\kappa > \kappa_s$, given in Section 5.2. As predicted in that section, the partial diffusion theory fluxes are less than the corresponding transport theory fluxes at large x. For water, the FARS data library shows that $\sigma_{1\ g\to g} < \sigma_{1,g}$ and hence, from Equations (5) and (7), it is apparent that $D_g(\text{DDT}) < D_g(\text{DT})$. Substitution into Equation (20), remembering that $\kappa_d^2 = (1-c)\sigma/D$, reveals that $\phi_d(\text{DDT}) < \phi_d(\text{DT})$, as found in the numerical calculations. This analysis can also be used to explain the errors in the partial diffusion theory fluxes obtained in the concrete and iron-water shields; in both of these, the neutron flux attenuation is governed by the high energy ($E > 0.5$ MeV) neutrons.

The agreement of the partial P_1 and partial DT theories, which is considerably better than the agreement of either one with the partial DDT theory, indicates that the argument presented in Section 4 for the similarity of these two theories holds good for energies below 0.5 MeV. This is found to be so for each shield investigated.

The total P_1 and DDT theories give neutron fluxes which are much too small for large x, whereas the total DT fluxes are, by comparison, in good agreement with the transport theory fluxes. This good agreement is due to

a compensation of opposing errors in the DT calculation and it can be explained as follows. An analysis of the neutron transport through the water shield shows that, at large distances from the source ($x > 50$ cm), it is the neutrons with energy above about 5 MeV which determine the flux attenuation. Using the FARS cross section data, and the transport theory flux spectrum at $x = 50$ cm to perform a group condensation, the following one-group ($E > 5$ MeV) cross sections and diffusion coefficients are obtained:

$$\sigma = 0.12 \text{ cm}^{-1}$$

$$\sigma_a = 0.08 \text{ cm}^{-1}$$

$$c = 0.33$$

$$D(P_1) = [0.36 - 0.06]^{-1}\text{cm} = 3.3 \text{ cm}$$

$$D(DT) = [0.36 - 0.18]^{-1}\text{cm} = 5.6 \text{ cm}$$

$$D(DDT) = [0.36 - 0.05]^{-1}\text{cm} = 3.2 \text{ cm}$$

It is apparent that the too large an anisotropic scattering correction used in the DT diffusion coefficient results in D(DT) being considerably larger than the 'correct' value $D(P_1)$. A one-group P_1 theory predicts a flux $\phi(P_1) \propto \exp(-\kappa(P_1)x)$, to be compared with the transport theory prediction of a flux $\phi \propto \exp(-\kappa x)$. For $c = 0.33$, Tait [1964b] gives $\kappa(P_1) \triangleq 1.4\ \kappa$, so the P_1 flux decreases much more quickly than the transport theory flux. Now $\kappa(DT) = [D(P_1)/D(DT)]^{\frac{1}{2}}\ \kappa(P_1) = 0.77\ \kappa(P_1)$, so $\kappa(DT) \triangleq 1.1\ \kappa$ and the DT flux decreases only slightly faster than the transport theory flux. Thus, for the water shield, the overcorrection for anisotropic scattering in the DT theory helps to compensate for the excessively large value of κ predicted by diffusion theories for materials with a large effective absorption. A similar, but smaller, compensation is noted for the concrete and iron-water shields.

7.2 The Concrete Shield

Partial P_1 and partial DT predict neutron doses which are about 1 per cent too low for $x > 40$ cm. Partial DDT predicts doses which are about 5 per cent too low for $x > 40$ cm. Apart from magnitude, the PD values for the dose are similar to those for the thermal flux shown in Figure 4; the errors in the thermal flux are about three times those in

the dose. The gamma dose is predicted to better than 1 per cent in the partial P_1 and partial DT calculations, but the partial DDT values are about 8 per cent too low for x > 40 cm.

The neutron dose RATIO values given by the total diffusion theories are shown in Figure 5. P_1 and DDT give similar results which are too small for x > 30 cm. The DT values show a similar trend, but are more accurate than the P_1 or DDT values. The thermal fluxes exhibit the same pattern, but have slightly smaller errors. The gamma-ray dose PD values given by the total diffusion theories are shown in Figure 6. They follow the trends obtained for the neutron dose and thermal flux, but have much smaller errors; this good accuracy is obtained because the gamma-ray average mean free path is larger than the neutron flux average relaxation length for the concrete examined here.

7.3 The Graphite Shield

Both the partial and total diffusion theory calculations give neutron doses which are very accurate, with errors of a few per cent near the source and less than 1 per cent for x > 40 cm. An examination of the neutron flux in graphite shows that when x > 50 cm, more than 99 per cent of the neutron dose comes from the thermal flux contribution. As the diffusion theory approximation is accurate for thermal neutrons in graphite, the good dose results obtained are to be expected. The partial diffusion theories predict the epithermal flux quite accurately, with ϕ_{28} being only 3 per cent too low at x = 180 cm.

As is seen in Figure 7, the total diffusion theories badly underestimate the fast neutron flux ϕ_f. This is due to the rapid removal of neutrons from the flux above 5 MeV by elastic scattering and, to a smaller extent, by inelastic scattering; this results in a large effective absorption cross section for this flux and, as this flux predominantly determines the behaviour of ϕ_f, too large a flux attenuation is predicted by diffusion theory. The RATIO values for ϕ_{28} do not decrease quite as quickly as those for ϕ_f; they are about four times as large as the ϕ_f RATIO values at x = 180 cm, but are still much too small once x > 60 cm.

7.4 The Iron Shield

The PD values for the neutron doses predicted by the partial diffusion theories are shown in Figure 8. The accuracy given by all three theories is quite good, except for large x, when the doses become too low. The thermal fluxes and the gamma-ray doses show PD values similar to the dose ones. Owing to the short relaxation length for gamma-rays in iron,

the gamma-ray flux has a spatial variation similar to that of the gamma-ray source, which is dependent upon the neutron flux.

The PD values for the neutron doses predicted by the total diffusion theories are shown in Figure 9. Once again the thermal and gamma-ray fluxes have PD values similar to those for the dose. It is apparent, from Figures 8 and 9, that the errors in the partial and total diffusion theory predictions of neutron dose, thermal flux and gamma-ray flux are small, at least for $x < 100$ cm. However, the RATIO values for the fast flux $\phi_f(E > 1 \text{ MeV})$, shown in Figure 10, indicate that the total diffusion theories underestimate ϕ_f for large x. As would be expected from these results, most of the contribution to the neutron dose in iron comes from neutrons with energies below 1 MeV; more specifically, for $x > 20$ cm, over 80 per cent of the dose comes from neutrons with energy below 0.5 MeV.

In the iron shield, the DDT fluxes tend to be slightly larger than either the P_1 or DT fluxes, and they are therefore more accurate for large x. This reversal in the usual trend of $\phi(DT) > \phi(DDT)$ is probably because, for the group structure used here, $\sigma_{1,g} < \sigma_{1,g\to g}$ in iron for energies below 3 MeV, thus reversing the argument put forward in Section 7.1.

7.5 The Iron-Water Shield

The PD values for the neutron doses predicted by the partial diffusion theories are shown in Figure 11. The PD values for the thermal fluxes have a similar pattern but are, on average, about twice as large. The errors in the gamma-ray dose are much less oscillatory and tend to a fairly constant value of about -3 per cent for the partial P_1 and DT theories and about -10 per cent for the partial DDT theory.

As can be seen from Figure 12, the values of the neutron dose given by the total diffusion theories are much too small for large x. The DT doses are reasonable for $x < 40$ cm and are considerably better than the P_1 or DDT values. The thermal flux exhibits the same trends. The PD values for the gamma-ray doses predicted by the total diffusion theories are shown in Figure 13. The DT values are once again the most accurate.

From these results, it is apparent that it is the transport of neutrons with energies above 0.5 MeV which determines the values of the neutron flux, and that it is the accuracy with which each theory evaluates the neutron transport in the water which determines the accuracy of that theory for the whole shield.

8. CONCLUSIONS

The partial diffusion theory calculations, which use transport theory

for the flux above 0.5 MeV and diffusion theory for lower energies, show that P_1 theory generally gives fluxes which are slightly more accurate than DT fluxes, but considerably more accurate than those given by DDT; the P_1 and DT theories predict fluxes which are accurate to within a few per cent whereas the DDT fluxes have errors of up to 20 per cent. All of the diffusion theory flux values are found to be too low at sufficient distances from the source; this behaviour has been predicted using a simple one-group analysis.

The total diffusion theory calculations, which use diffusion theory to evaluate the neutron flux at all energies, are almost all found to be deficient for the evaluation of the fast flux ($E > 1$ MeV) in the shields studied here. They give a fast flux which is attenuated too quickly by the shield. With the exception of the flux in the iron shield and the thermal flux in graphite, the neutron flux below 1 MeV tends to be dependent on the flux above this energy, and so the flux below 1 MeV is also underpredicted by the total diffusion theory calculations.

There are three exceptions to this trend of underprediction of the neutron flux by the total diffusion theories. The thermal flux in graphite is predicted extremely well by all diffusion theories; the flux in iron below about 0.5 MeV is predicted fairly well by all diffusion theories; and the neutron flux in water is predicted with fair accuracy, especially in comparison with the P_1 and DDT values, by the DT calculations. The first two exceptions follow simply from the adequacy of all diffusion theories in these cases, but the accuracy of DT for water occurs because an excessively large correction for anisotropic scattering compensates for the error introduced into diffusion theory by a large effective absorption cross section for the high energy neutrons (which determine the flux attenuation), resulting in a fairly accurate predicted flux. This compensation of errors is also evident in the other shields which contain hydrogen, that is, in the concrete and iron-water shields. In these shields, the DT calculated fluxes are still too low at large distances into the shields, but they are appreciably more accurate than either the P_1 or the DDT fluxes.

The accuracy of a diffusion theory which neglects the effects of anisotropic scattering has not yet been considered. However, from the analysis in Sections 4 and 5 and from the multigroup results in Section 7, it can be deduced that, for x sufficiently large, such a theory would lead to fluxes which were smaller, and hence less accurate, than those predicted by either P_1, DT or DDT.

To summarise, given the correct neutron flux above 0.5 MeV, both P_1 and DT give accurate values for the flux below 0.5 MeV in the shields investigated here. This indicates that the non-removal flux component which comes from the scattering of removal neutrons in the shield is accurately evaluated by P_1 or DT theory for energies below 0.5 MeV. The non-removal flux also has a component which enters the shield through its boundaries. The high energy part of this flux, in particular, tends to be badly underpredicted at large distances into the shield by all diffusion theories unless the shield contains a large proportion of hydrogen, in which case DT gives reasonable flux values. It is therefore recommended that the most common form of diffusion theory, which incorporates the transport approximation to correct for anisotropic scattering, be used in removal-diffusion calculations.

It is apparent from this investigation that one should be careful with the use of removal-diffusion theory in situations where the high energy (E > 0.5 MeV) neutron flux incident on the shield boundaries is predominantly non-removal flux. In this case, the diffusion theory used will tend to predict too large an attenuation of the flux and hence underestimate the high energy neutron flux in the shield and, depending on the shield material, perhaps the low energy neutron flux as well.

9. REFERENCES

Bell, G.I. & Glasstone, S. [1970] - Nuclear Reactor Theory, Van Nostrand Reinhold Company, New York, Chap. 4.

Bell, G.I., Hansen, G.E. & Sandmeier, H.A. [1967] - Multitable Treatment of Anisotropic Scattering in S_N Multigroup Transport Calculations, *Nucl. Sci. Eng.*, 28:376.

Engle, W.W. Jr. [1967] - ANISN, A One-dimensional Discrete Ordinates Transport Code with Anisotropic Scattering. K-1693.

Pendlebury, E.D. & Underhill, L.H. [1962] - Physics of Fast and Intermediate Reactors, IAEA Vienna, Vol. III, p.73.

Ponti, C. & Van Heusden, R. [1974] - SABINE-3. EUR 5159.

Price, B.T., Horton, C.C. & Spinney, K.T. [1957] - Radiation Shielding, Pergamon Press, London, 175.

RSIC Computer Code Collection [1969] - FARS, 122-group Coupled Neutron and Gamma-ray Transport Code Cross-section Data. DLC-9.

Sahin, S. [1973] - Comparison of Transport and Diffusion Theory for Fast Reactor Shielding Calculations, *Atomkernenergie*, 22:24.

Tait, J.H. [1964a] - An Introduction to Neutron Transport Theory, Longmans, London, p.27.

Tait, J.H. [1964b] - *op. cit.*, p.53.

Tanaka, Y., Suzuki, I. & Ontani, N. [1972] - The Development of the Two-dimensional Shielding Code RASC-2D and its Application. CONF-72018, Vol. 2, p.611.

TABLE 1

COMPOSITION OF THE SHIELD MATERIALS

Material	Element	Percentage by Weight	Density (g cm^{-3})
Water	H	11.2	1.00
	O	88.8	
Concrete	H	1.0	2.30
	O	50.0	
	Al	5.0	
	Si	30.0	
	Ca	10.0	
	Fe	4.0	
Graphite	C	100.0	2.25
Iron	Fe	100.0	7.86

TABLE 2

MULTIGROUP STRUCTURE FOR CONDENSED FARS CROSS SECTIONS

Neutron Group	Upper Boundary	Gamma-ray Group	Upper Boundary
1	15.0 MeV	1	10 MeV
2	13.5	2	8
3	12.2	3	6.5
4	10.0	4	5
5	8.19	5	4
6	6.07	6	3
7	4.07	7	2.5
8	3.01	8	2
9	2.23	9	1.33
10	1.65	10	1
11	1.35	11	0.6
12	820 keV		
13	500		
14	302		
15	183		
16	67.4		
17	24.8		
18	19.3		
19	9.12		
20	3.35		
21	1.23		
22	454 eV		
23	167		
24	61.4		
25	22.6		
26	8.32		
27	3.06		
28	1.13		
29	0.414		

TABLE 3

THE SPATIAL VARIATION OF NORMALISED FLUX VALUES IN EACH SHIELD

Shield	x (cm)	Neutron Dose	Gamma-ray Dose	Fast Neutron Flux (E > 1 MeV)	Thermal Neutron Flux
Water	0	1.00 E+0	1.00 E+0	1.00 E+0	1.00 E+0
	25	7.23 E-3	2.87 E-1	6.94 E-3	1.54 E-2
	50	1.81 E-4	8.31 E-2	1.95 E-4	2.75 E-4
	75	7.54 E-6	2.59 E-2	8.52 E-6	9.58 E-6
	100	4.21 E-7	8.00 E-3	4.87 E-7	4.82 E-7
Concrete	0	1.00 E+0	1.00 E+0	1.00 E+0	1.00 E+0
	25	5.42 E-2	4.10 E-1	4.01 E-2	2.93 E-1
	50	3.73 E-3	7.10 E-2	2.76 E-3	2.50 E-2
	75	2.67 E-4	1.08 E-2	2.08 E-4	1.70 E-3
	100	2.05 E-5	1.78 E-3	1.66 E-5	1.20 E-4
Graphite	0	1.00 E+0	1.00 E+0	1.00 E+0	1.00 E+0
	50	1.67 E-1	4.96 E-1	1.93 E-3	4.59 E-1
	100	5.12 E-2	1.60 E-1	3.71 E-6	1.42 E-1
	150	1.56 E-2	4.91 E-2	1.21 E-8	4.36 E-2
	200	4.20 E-3	1.33 E-2	5.27 E-11	1.17 E-2
Iron	0	1.00 E+0	1.00 E+0	1.00 E+0	1.00 E+0
	25	1.89 E-1	2.91 E-1	2.46 E-2	6.96 E-1
	50	3.31 E-2	9.14 E-2	7.76 E-4	2.72 E-1
	75	5.18 E-3	2.25 E-2	2.55 E-5	7.38 E-2
	100	7.42 E-4	4.43 E-3	8.82 E-7	1.52 E-2
Iron-Water	0	1.00 E+0	1.00 E+0	1.00 E+0	1.00 E+0
	15	5.99 E-2	1.57 E+0	3.60 E-2	3.63 E+0
	25	1.04 E-2	2.55 E-1	8.47 E-3	2.80 E-1
	35	1.25 E-3	7.09 E-2	8.93 E-4	6.91 E-2
	45	2.59 E-4	1.41 E-2	2.37 E-4	5.51 E-3
	55	3.32 E-5	3.46 E-3	2.70 E-5	1.66 E-3
	65	7.83 E-6	8.18 E-4	7.69 E-6	1.44 E-4
	75	1.05 E-6	2.02 E-4	9.35 E-7	4.85 E-5
	85	2.73 E-7	5.27 E-5	2.84 E-7	4.45 E-6
	95	3.76 E-8	1.34 E-5	3.61 E-8	1.60 E-6
	105	5.71 E-9	9.97 E-6	7.36 E-9	1.27 E-7

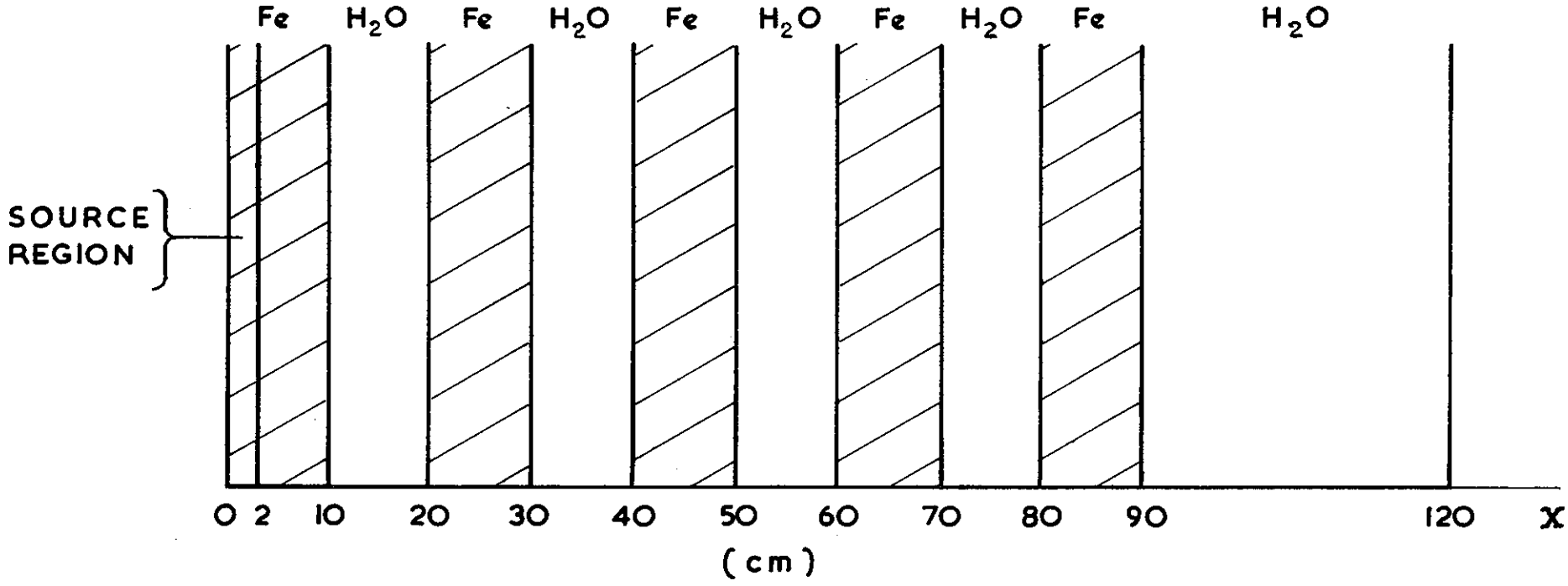

FIGURE 1. DIMENSIONS OF THE IRON-WATER SHIELD

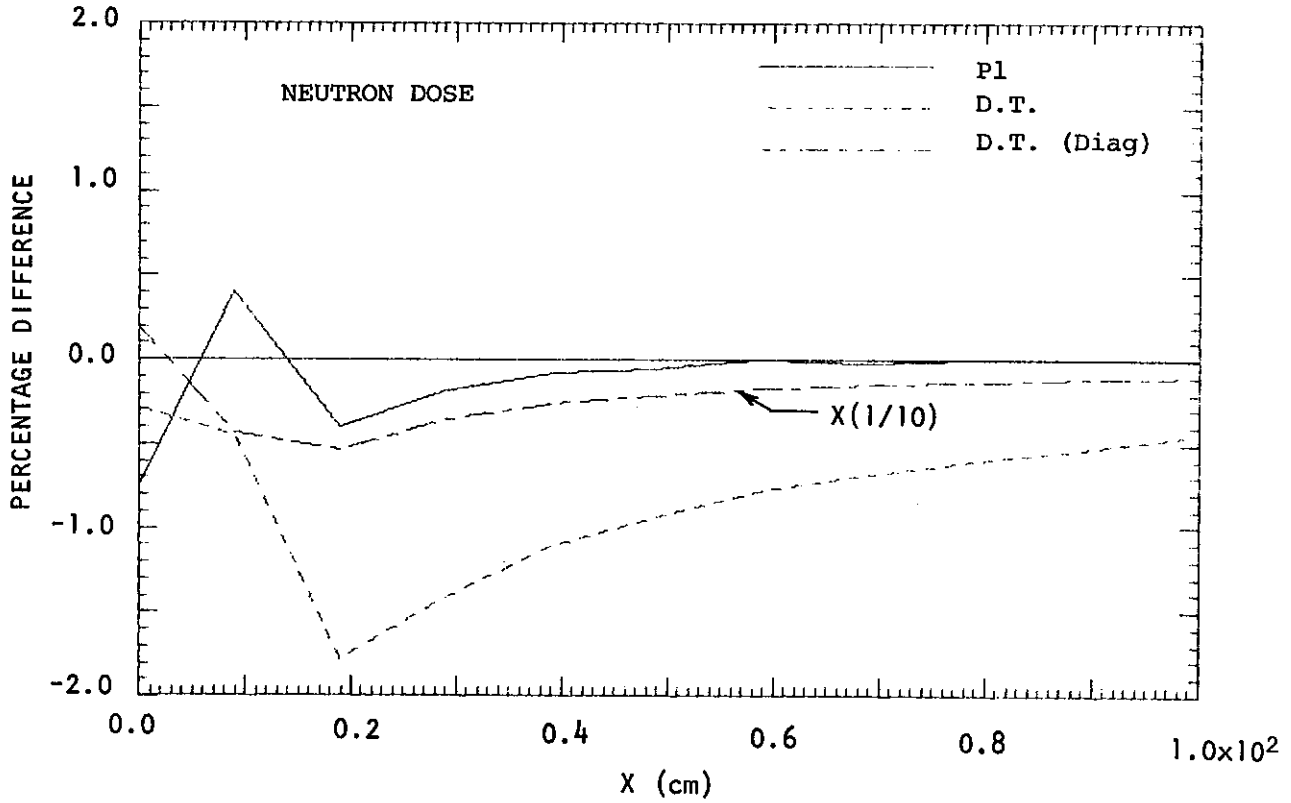

FIGURE 2. NEUTRON DOSE IN WATER: DIFFUSION THEORY USED FOR E < 0.5 MeV

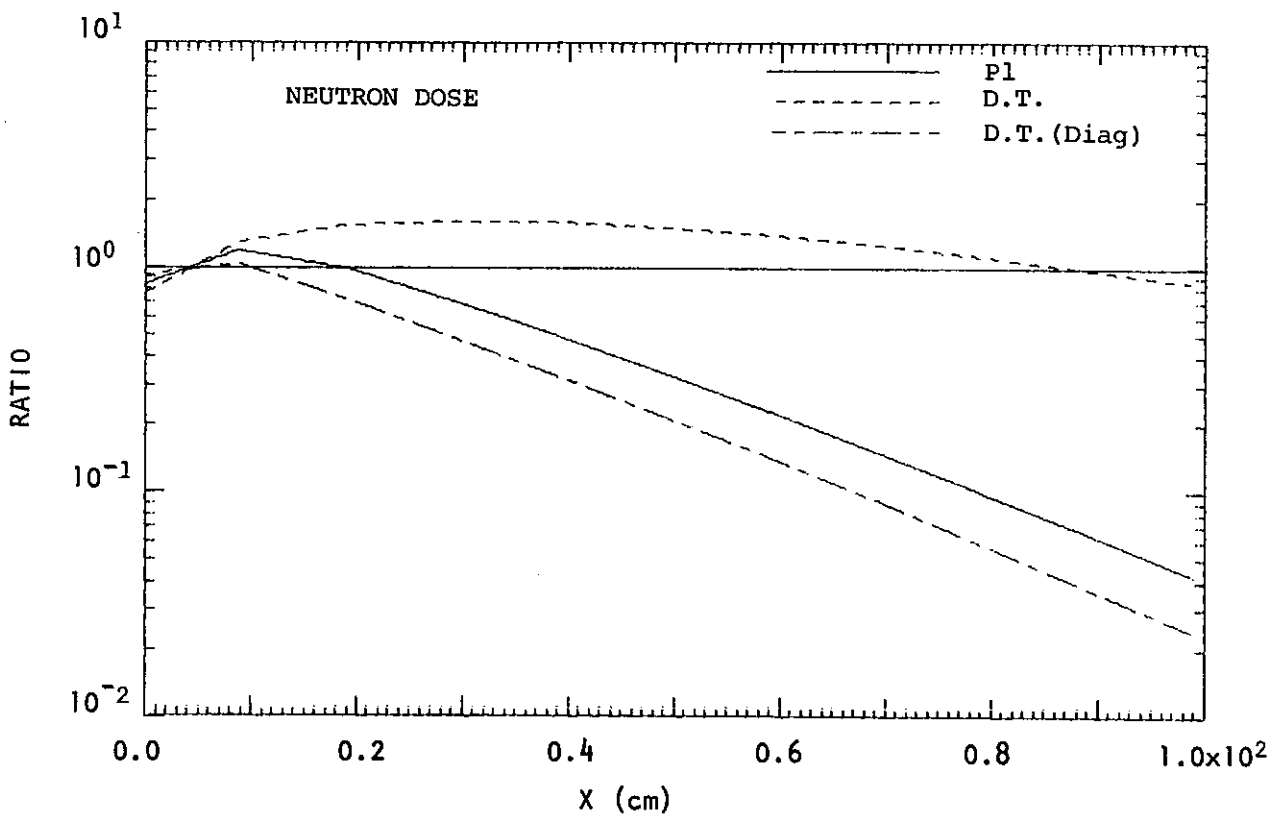

FIGURE 3. NEUTRON DOSE IN WATER: DIFFUSION THEORY USED FOR ALL E

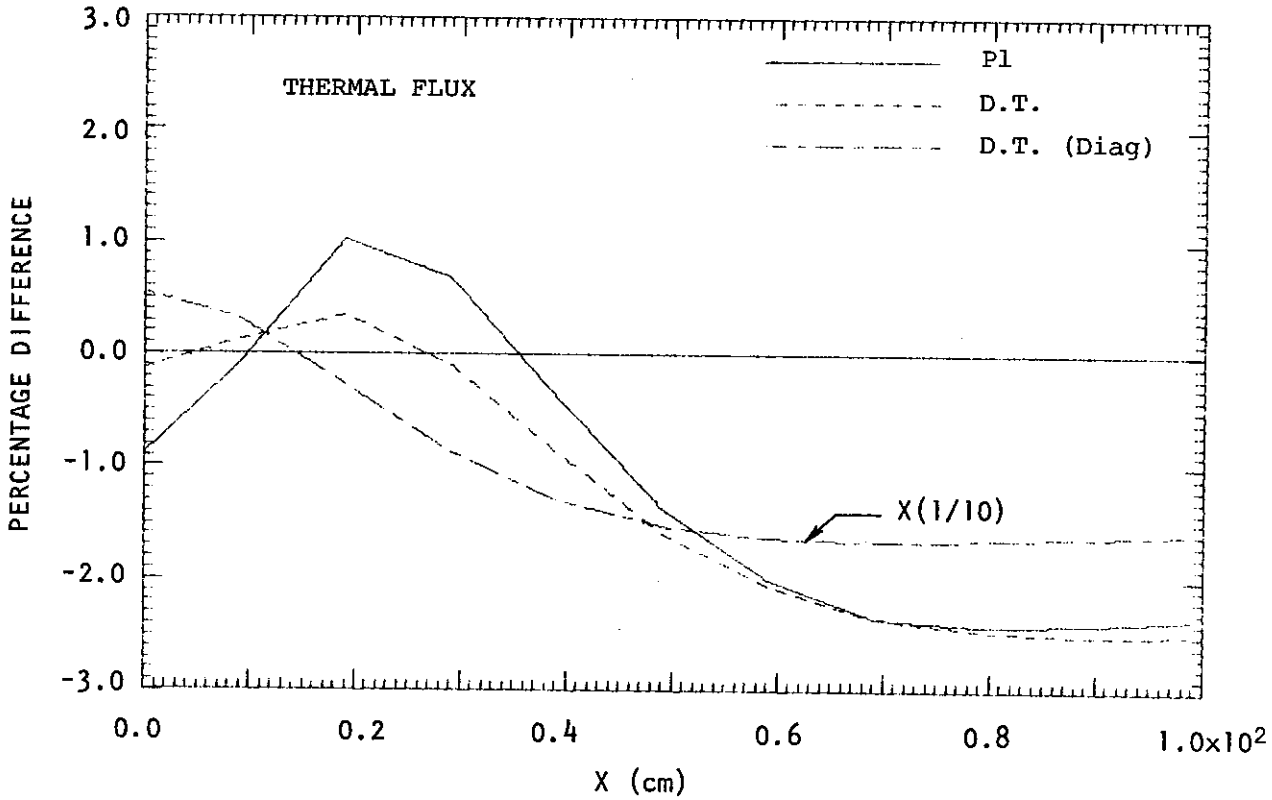

FIGURE 4. THERMAL NEUTRON FLUX IN CONCRETE: DIFFUSION THEORY USED FOR E < 0.5 MeV

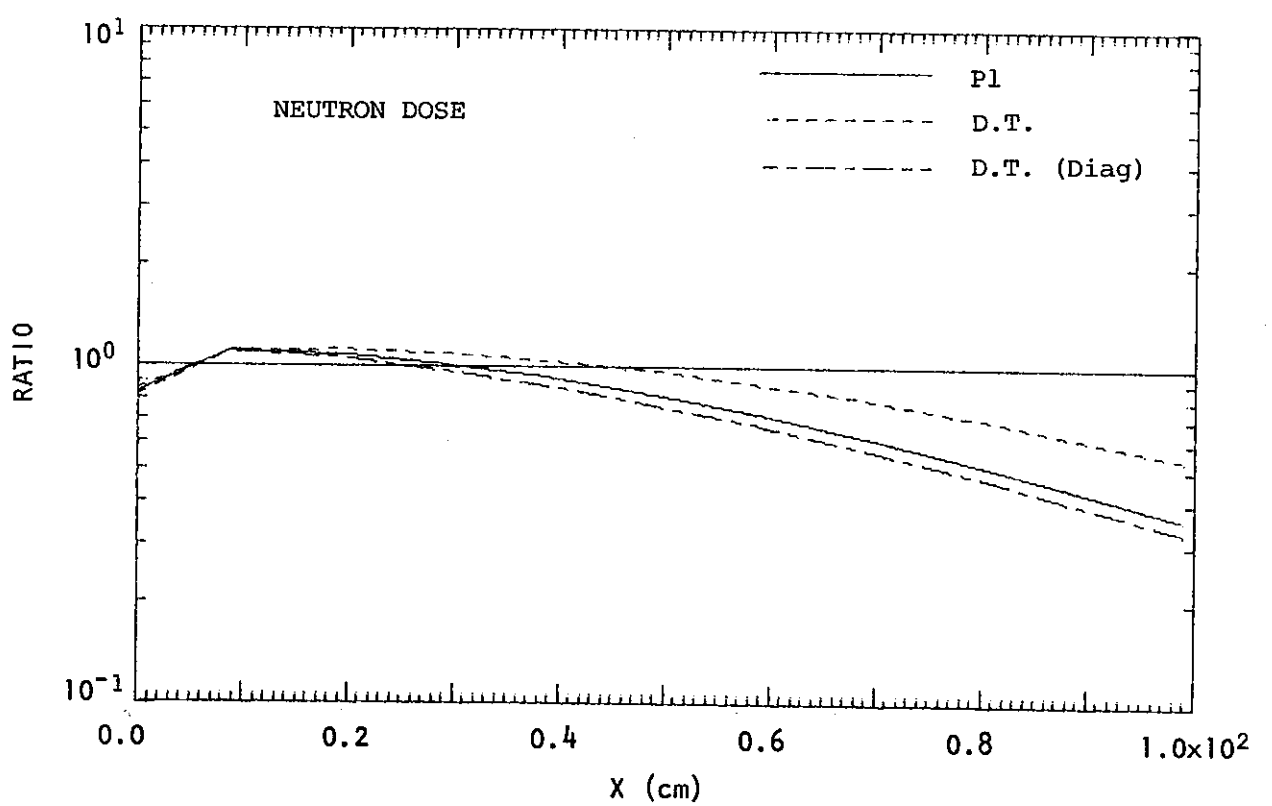

FIGURE 5. NEUTRON DOSE IN CONCRETE: DIFFUSION THEORY USED FOR ALL E

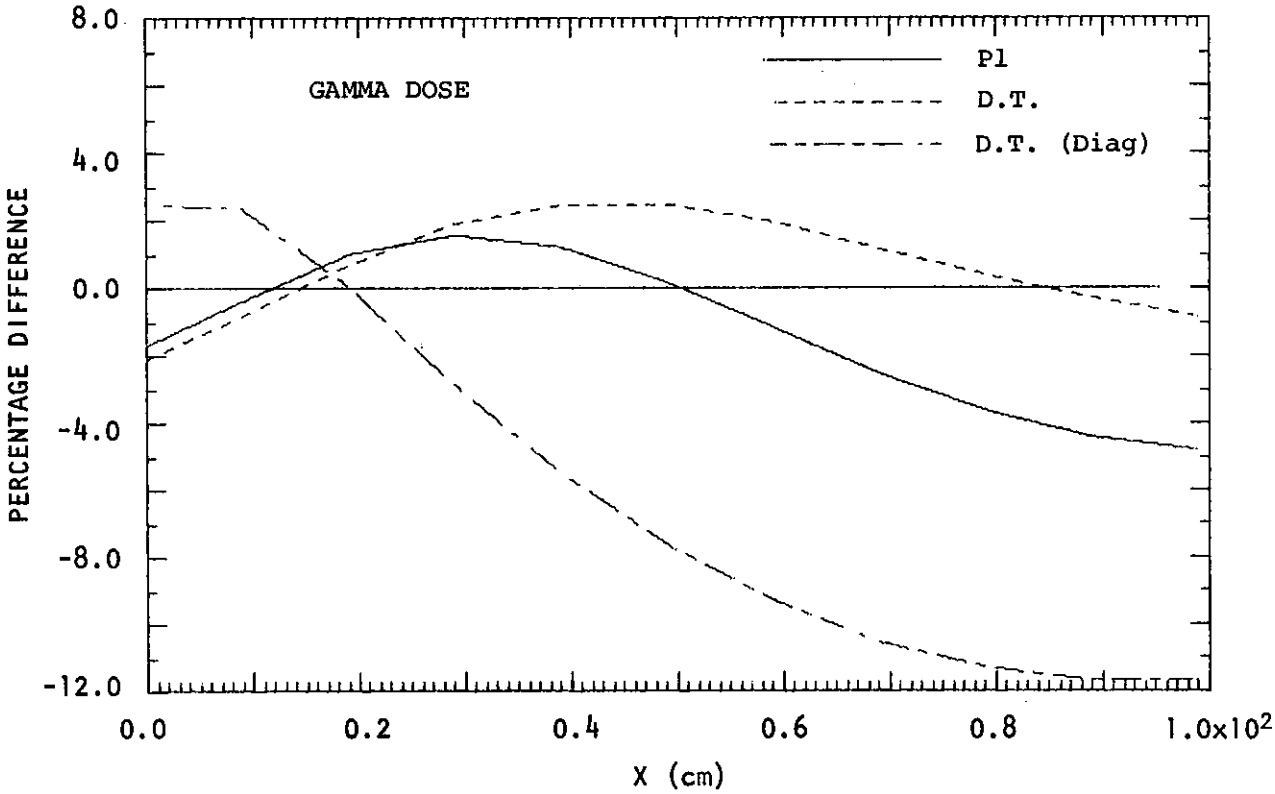

FIGURE 6. GAMMA RAY DOSE IN CONCRETE: DIFFUSION THEORY USED FOR ALL E

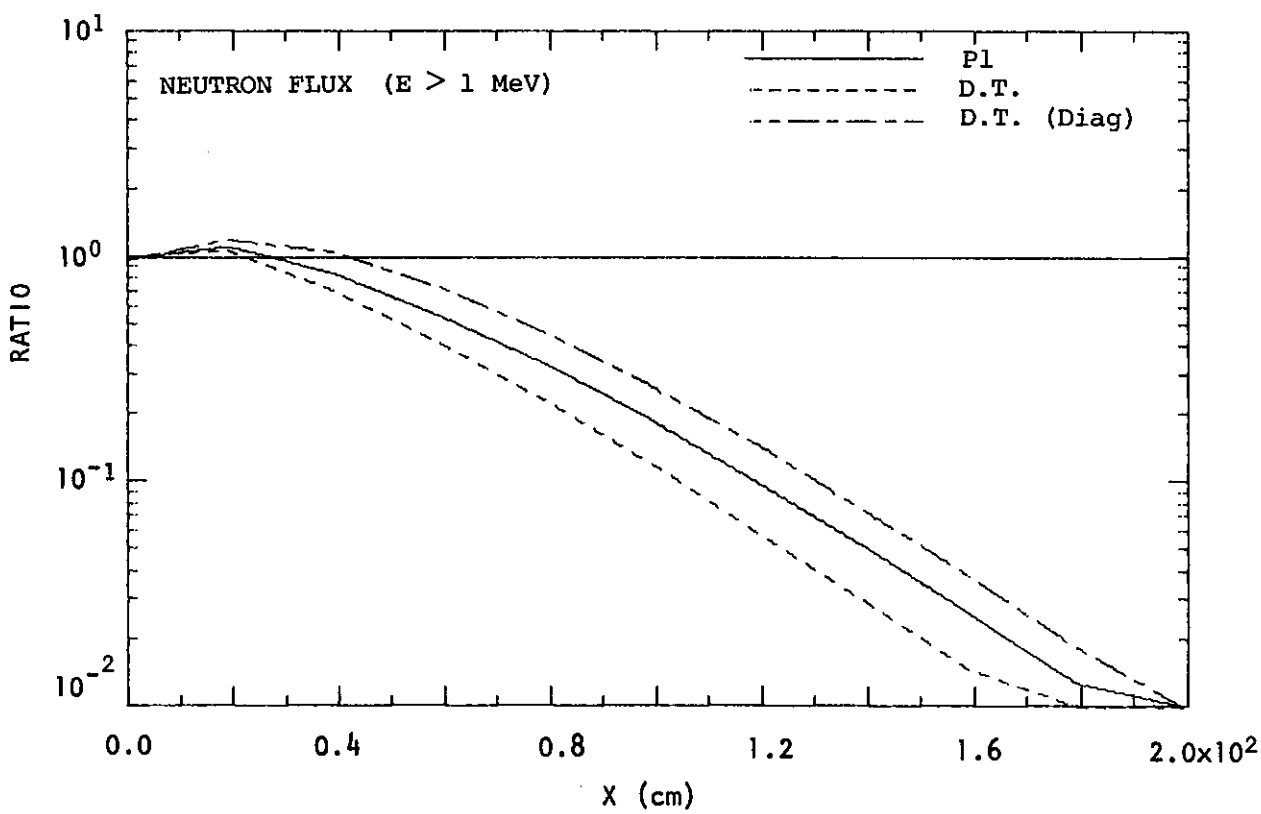

FIGURE 7. FAST FLUX IN GRAPHITE: DIFFUSION THEORY USED FOR ALL E

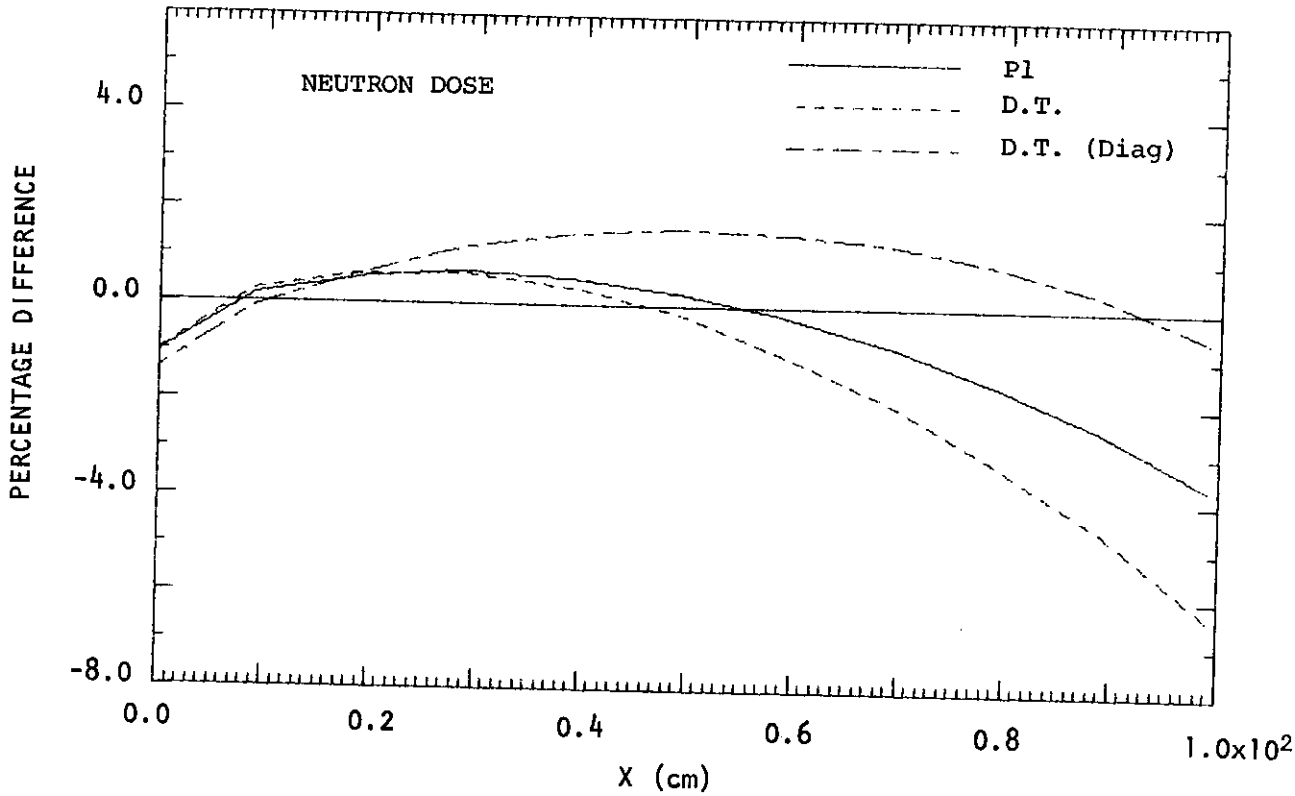

FIGURE 8. NEUTRON DOSE IN IRON: DIFFUSION THEORY USED FOR E < 0.5 MeV

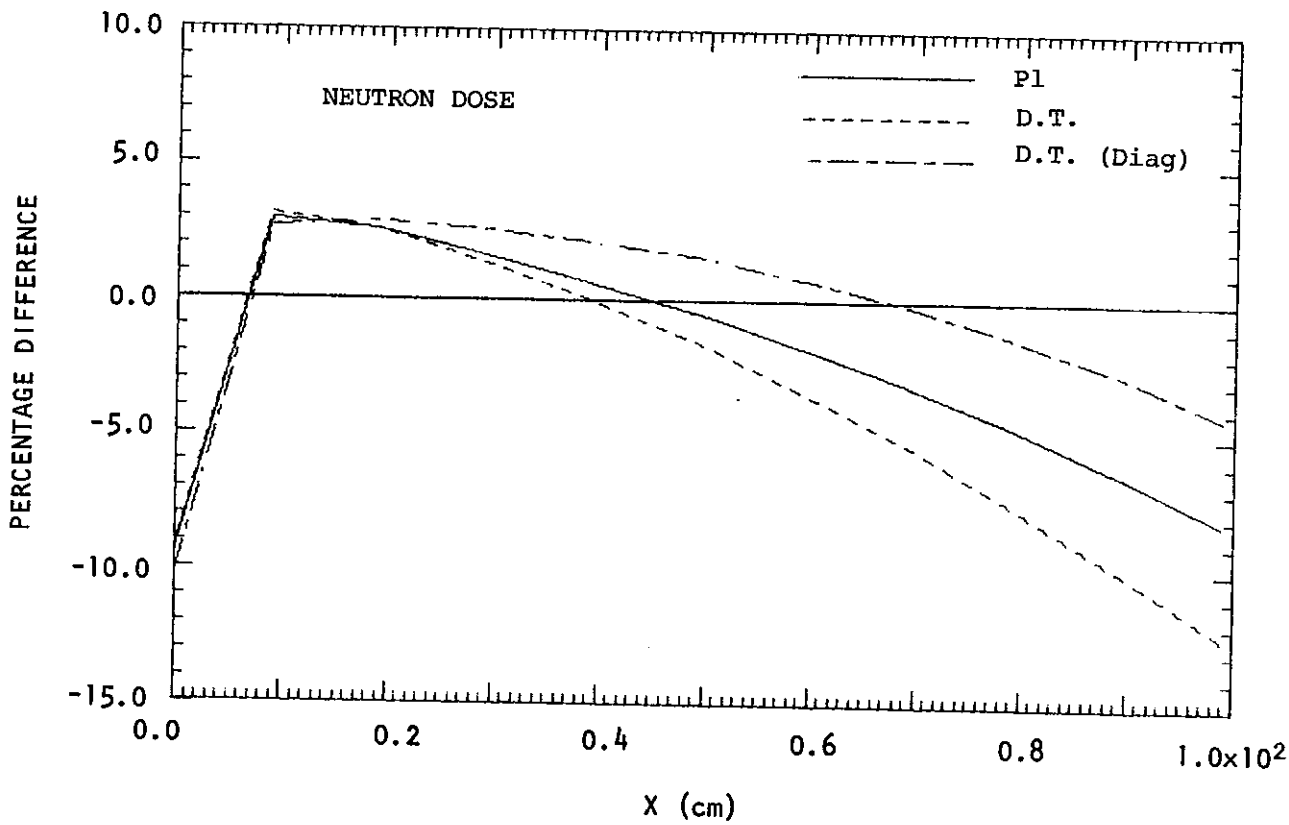

FIGURE 9. NEUTRON DOSE IN IRON: DIFFUSION THEORY USED FOR ALL E

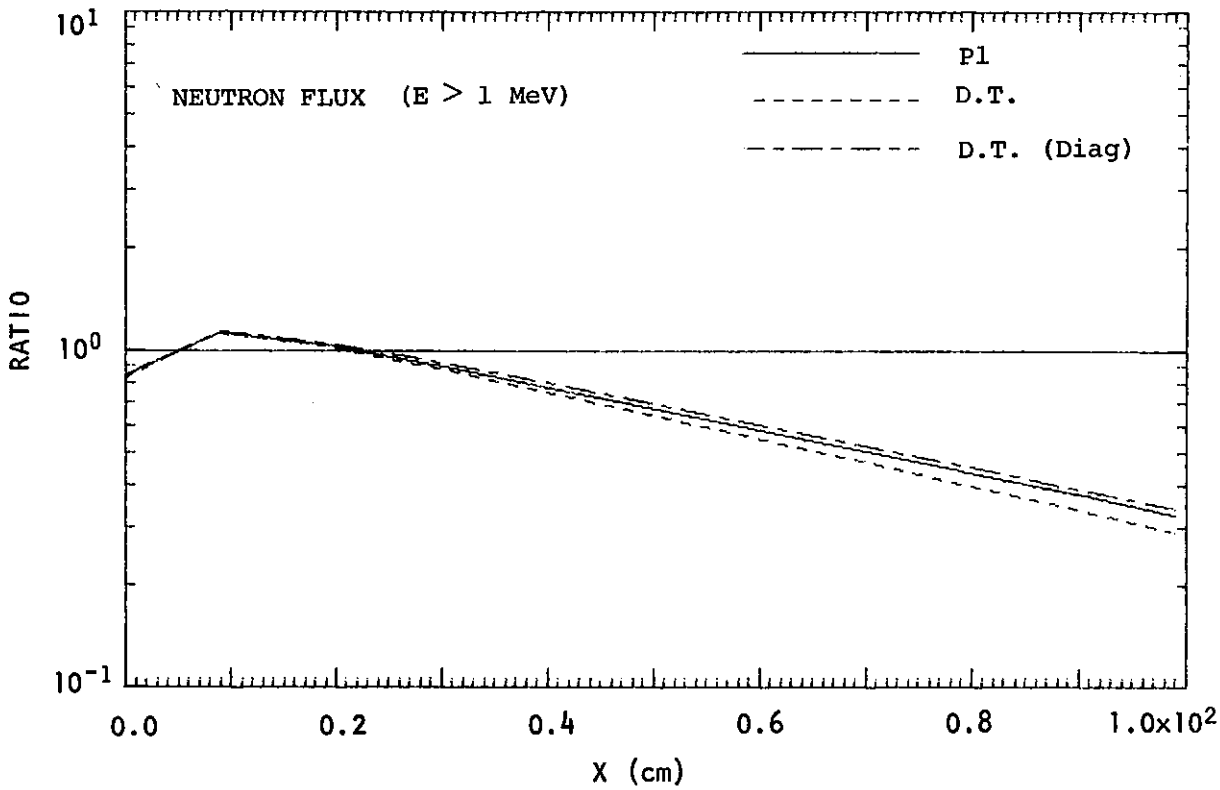

FIGURE 10. FAST FLUX IN IRON: DIFFUSION THEORY USED FOR ALL E

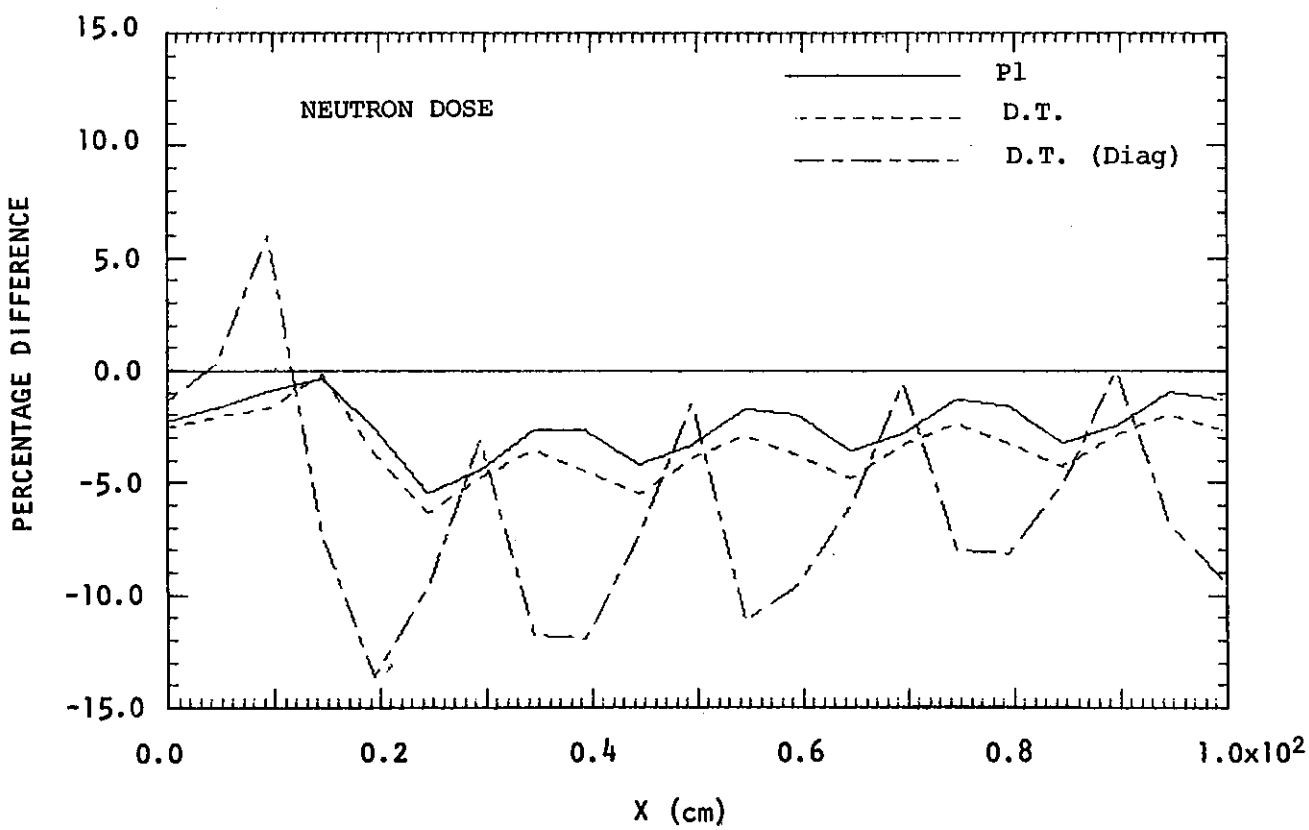

FIGURE 11. NEUTRON DOSE IN IRON-WATER SHIELD: DIFFUSION THEORY USED FOR E < 0.5 MeV

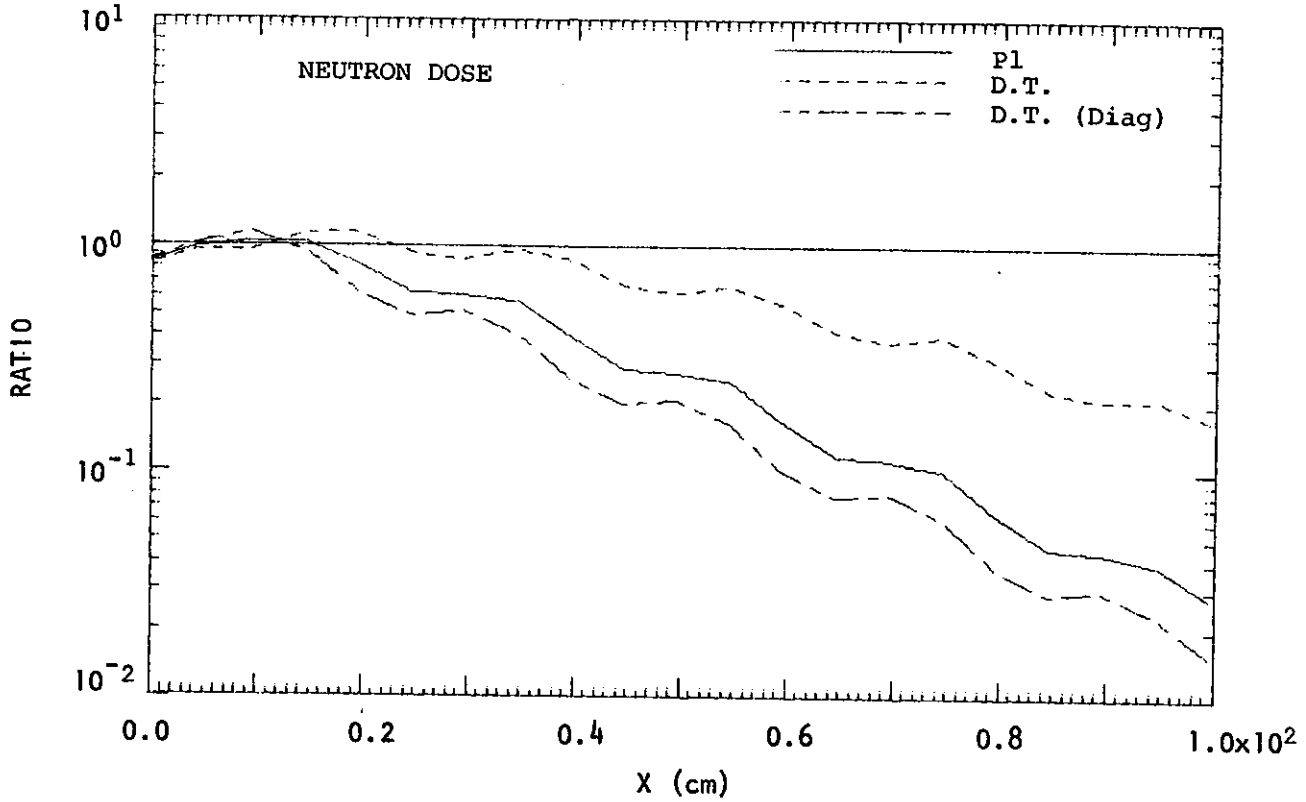

FIGURE 12. NEUTRON DOSE IN IRON-WATER SHIELD: DIFFUSION THEORY USED FOR ALL E

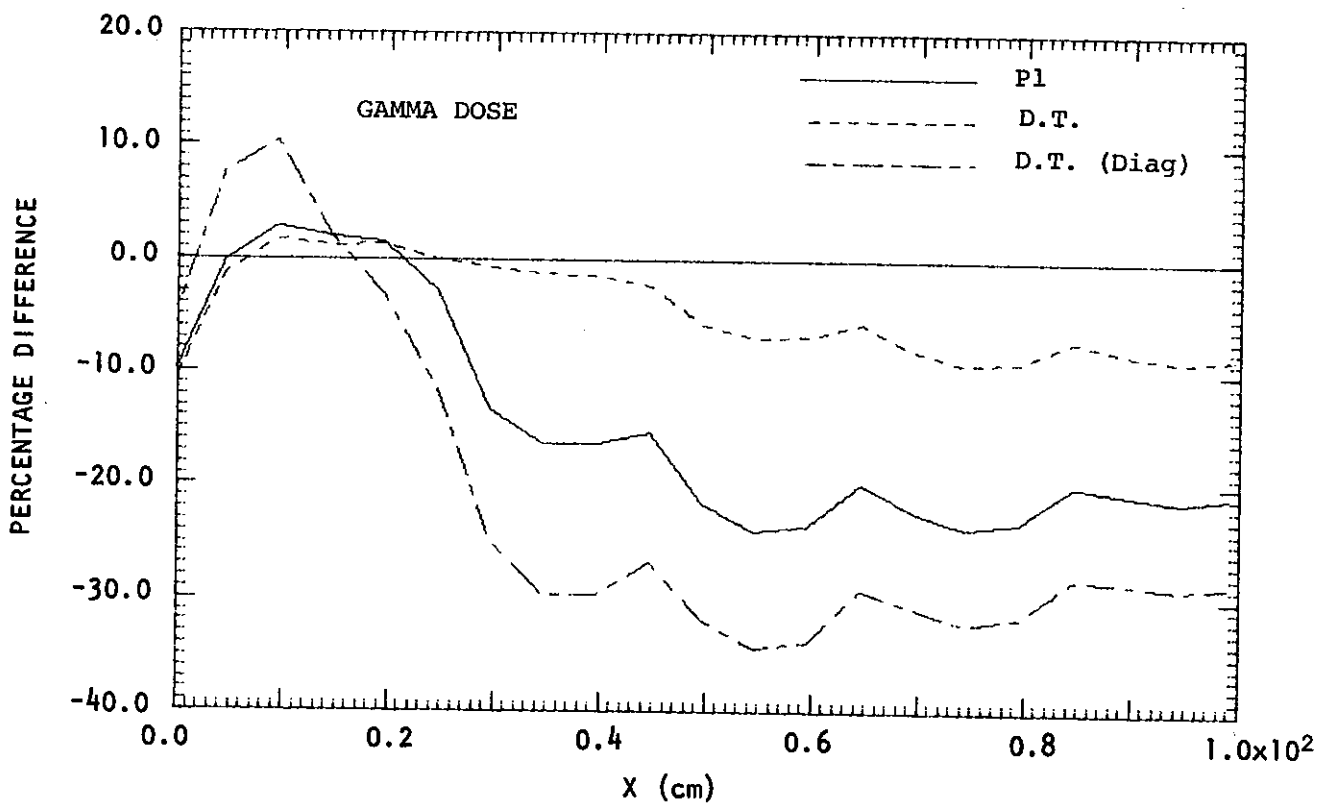

FIGURE 13. GAMMA RAY DOSE IN IRON-WATER SHIELD: DIFFUSION THEORY USED FOR ALL E